



## Article

# Automatic River Planform Recognition Tested on Chilean Rivers

Andrea Gianni Cristoforo Nardini <sup>1,\*</sup>, Francisca Salas <sup>2</sup>, Zoila Carrasco <sup>3</sup>, Noelia Valenzuela <sup>3</sup>, Renzo Rojas <sup>3</sup>, José Vargas-Baecheler <sup>2</sup> and Santiago Yépez <sup>3,\*</sup>

<sup>1</sup> Fundación CREACUA, Riohacha 440001, Colombia

<sup>2</sup> Departamento de Ingeniería Civil, Facultad de Ingeniería, Universidad de Concepción, Concepción 4070409, Chile; fransalas@udec.cl (F.S.); jvargas@udec.cl (J.V.-B.)

<sup>3</sup> Departamento Manejo de Bosques y Medio Ambiente, Facultad de Ciencias Forestales, Universidad de Concepción, Concepción 4070374, Chile; zcarrasco2016@udec.cl (Z.C.); nvalenzuela2016@udec.cl (N.V.); rerojas@udec.cl (R.R.)

\* Correspondence: nardiniok@gmail.com (A.G.C.N.); syopez@udec.cl (S.Y.)

**Abstract:** This paper addresses the issue of the automatic identification of river reaches and their planform type given the (observed) set of geomorphic elements and units. It introduces further advances with respect to the original proposal by Nardini and Brierley, and it explores explicitly the ability of the algorithm and associated tools to work properly on significantly different rivers while adopting a given same parametrization. This was indeed an envisaged ability speculated as a challenging conclusion of the previous work. The Duqueco, Laja, and Biobío rivers (Chile) were analyzed for this purpose. The conclusion is definitely positive, which opens future promising application horizons.

**Keywords:** river planform; river reaches; automatic identification; geomorphic elements and units; Biobío basin



**Citation:** Nardini, A.G.C.; Salas, F.; Carrasco, Z.; Valenzuela, N.; Rojas, R.; Vargas-Baecheler, J.; Yépez, S. Automatic River Planform Recognition Tested on Chilean Rivers. *Water* **2023**, *15*, 2539. <https://doi.org/10.3390/w15142539>

Academic Editor: Tomasz Falkowski

Received: 4 June 2023

Revised: 2 July 2023

Accepted: 5 July 2023

Published: 11 July 2023



**Copyright:** © 2023 by the authors. Licensee MDPI, Basel, Switzerland. This article is an open access article distributed under the terms and conditions of the Creative Commons Attribution (CC BY) license (<https://creativecommons.org/licenses/by/4.0/>).

## 1. Introduction

One of the key characters of a river is its “planform”; i.e., its spatial configuration in terms of path, sinuosity, number of channels and their width, and the assemblage of in channel geomorphic units. It is also the core of several geomorphic classification schemes (e.g., Kondolf et al. [1], Buffington and Montgomery [2], and Brierley and Fryirs [3]). Nardini et al. [4] adopted the planform as one of the key attributes to segment a river into meaningful stretches.

The ability to automatically identify planform types would bring several benefits; namely: (i) it would greatly reduce the characterization effort particularly for large size basins; (ii) it would ensure consistency, while relying on expert judgment definitely is affected by subjective perception; and (iii) it would support a systematic monitoring of the evolution of rivers. All this is certainly of great interest considering that the geomorphic units found in a river at a certain moment are not fixed elements but typically manifestations of a character and behavior that is dynamic and ever-changing. Climate change is introducing a further dimension to this pattern of change.

Curiously, in the literature several attempts can be found to automatically identify the geomorphic elements (valley bottom and active channel) and units (e.g., bars, islands, and water channels) from remotely sensed data (e.g., Parker et al. [5], Piégay et al. [6], Ouellet et al. [7], Demarchi et al. [8], Bernard et al. [9], and Jézéquel et al. [10]). However, we have not found attempts to identify the planform typology automatically once such elements are given based on a direct observation on the territory, be it through a manual, expert-based procedure or an automatic one. The only work directly addressing this challenge, as far as we know, is that of Nardini and Brierley [11].

Similar exercises utilized supervised machine learning (ML) algorithms to identify the planform based on some “predictors” (causal factors) in order to extrapolate then to

broad territories (e.g., Frasson et al. [12], Beechie and Imaki [13], Beechie et al. [14], and Rabanaque et al. [15]); however, although some predictors are very close to some of the geomorphic attributes describing planforms, they mainly refer to different things, and in any case they are not conceived to directly constitute the set of planform descriptors. Also, the belonging to a given planform category is performed manually based on an expert judgment rather than an automatic procedure. Other attempts (e.g., Bertrand et al. [16], Guillon et al. [17], and Horacio et al. [18]) were rather based on unsupervised ML algorithms, where reaches were described by a set of attributes (quantified by indicators) and then grouped into clusters of similar elements finally assigned—again based on expert judgment—to the different planform typologies. There, attributes are calculated on pre-defined stretches, although the final reaches may not coincide with them, which may create a discrepancy. Although implemented through a different technique (namely, the Self-Organizing Maps (SOMs)), the experience of Bizzi and Lerner [19] is conceptually similar, working again on pre-defined stretches. Perhaps an exercise more similar to the one we address here is the attempt to recognize the type of drainage network (terrestrial or even extraterrestrial), again through supervised ML but this time fed by (remotely sensed) images (Donadio et al. [20]). This is, however, a global judgment over a whole network and lies clearly far from our problem both due to the (lacking) detail of the attributes considered and because it does not address the difficult associated problem of recognizing jointly both the type and the spatial reach where it applies. Additionally, the idea of applying a supervised ML algorithm to a set of images (the assemblage of geomorphic elements and units directly observed for a river) faces the harsh difficulty of counting with a (very) large number of examples classified manually (analogously to the exercise of the “River Zoo” (<http://dame.oacn.inaf.it/riverzoo.html>, accessed on 15 February 2023)).

Nardini and Brierley [11] defined a set of planform archetypes, then chose a set of attributes to characterize them according to explicit criteria together with suitable indicators computed for each one of the river “slices” produced by a discretization process (according to the Fluvial Corridor Toolbox scheme by Alber and Piégay [21]). These indicators are then transformed by suitable scalar Value Functions (VFs) fully defined by a set of parameters to be specified that translate the value of each indicator into a judgment of adherence to a given criterion. For each archetype, a collage of such VFs is defined that composes a specific multi-attribute VF: they all are evaluated in parallel for each slice, and the archetype for which the corresponding multi-attribute VF assumes the highest score is the “winner”; i.e., is assigned to that slice. This process is permeated by the idea of evaluating the attributes over a moving window centered on the current slice  $i$ , where such a window has a length proportional to the local active channel (AC) width to always guarantee a suitable holistic view rather than a reductionist one while adapting to a spatially changing river. Here, for the AC, we mean the low-flow channels together with all the bars (excluding islands) according to Nardini et al. [22]. This algorithm was applied to the Baker River (Southern Chile) with promising results [4]. This Excel<sup>®</sup> spreadsheet (programmed) that implemented the algorithm described here is referred to as the “Tool”.

A fundamental doubt was however raised; i.e., whether the chosen parametrization (the set of values assigned to the parameters) for the Baker River also would serve well for other significantly different rivers (or, in other words, whether the good performance was due to an overfitting of the parameters). This paper is the fruit of research explicitly aimed at exploring the truthfulness of this thesis by applying the same Tool with the same given parametrization to a set of three rivers that are very different in terms of size and characteristics but all located in the VIII Region (south-central area) in Chile.

## 2. Methodology

The methodology adopted here was the same as already described in Nardini and Brierley [11] (already synthesized above), but it included some further progress described in what follows.

### 2.1. Ability to Deal with Rivers with Highly Variable AC Width

Some of the rivers considered here display a peculiarity: their width greatly and suddenly varies along the river, as can be seen, for example, in the Duqueco case in the segment between slices n. 1000–1500 (Figure 1). This constitutes a difficult challenge for the Planform algorithm (which is based on the concept of significant length) because, while in the narrow segment it is quite short, as soon as a wide segment is touched, it suddenly becomes very large, and as such it tends to ignore the character of the widened but proportionally short segment.

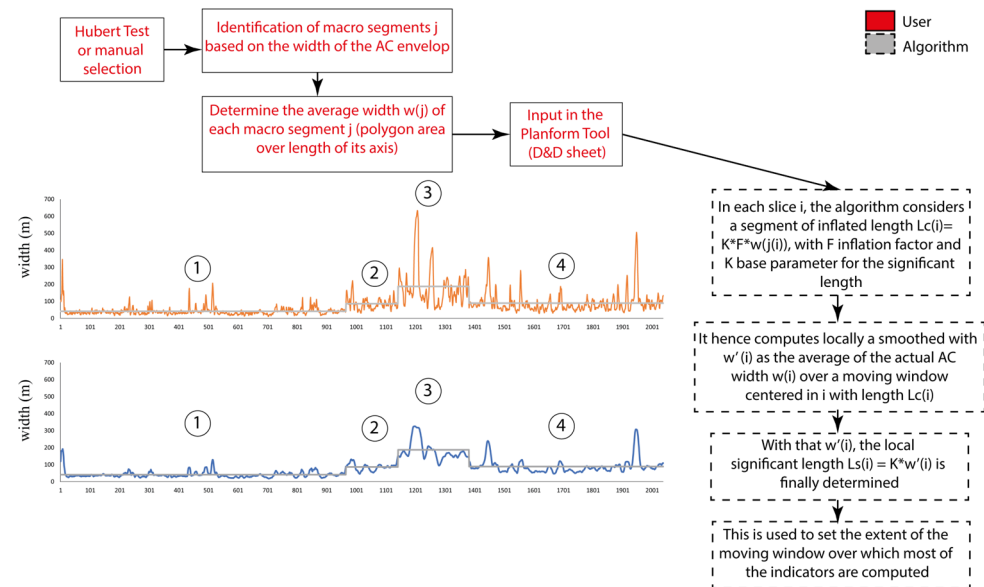


**Figure 1.** The algorithm introduced to manage highly varying AC width situations. This example (Duqueco River) shows how this process works: the grey line in the two graphs identifies macro segments (4 from the Hubert test) and determines their width  $w(j)$ ; the orange line (first graph above) is the original AC width (varying greatly); the blue line (graph below) is the output width, which is quite smoothed although still sensitive to AC width variations. The actions performed by the user are in red text, while those performed by the algorithm are in black. Numbers (1, 2, ...) identify some characteristic sections to point out how the AC width is modified by this algorithm.

To address this issue, we introduced a step to smooth out this width variability. To achieve that, the idea was first to identify macro segments over which to determine a local average AC width; this was used to determine the length of a moving window (for all the slices falling within that macro segment) over which the actual average AC width was determined (denoted as “smoothed”); this was in turn used to determine the local  $L_C(i)$  with which the moving window was created. The macro segments can be identified manually or via the AGO creation criterion introduced by Alber and Piégay [21] based on the Hubert test (Hubert [23]); clearly, this includes an arbitrary step because the user must specify how many diverse segments are to be obtained, as the Hubert test just finds where they are. However, reasonable low numbers (like 3 or 5) work well. This new part of the overall algorithm is depicted in the following Figure 1; in case only one Hubert segment was adopted together with a unity inflation factor,  $L_C$  is the whole river and  $w(j(i))$  is the average river width.

### 2.2. Improvement of Some Indicators and Value Functions (VF)

With respect to the original Baker exercise described in Nardini and Brierley [11], a number of improvements were introduced that are briefly summarized below; they refer to:

- Adjustments or refinement of Value Functions (definition, attributes, and their parameter values);

- Determination of sinuosity;
- Constrained sinuosity conditions;
- Adoption of multiplicative scalar Value Functions (VFs).

In the original Baker exercise, some archetypes, though considered in the algorithm, were not called into play because they were not present in that river. As such, they were not tested. Other posterior applications showed that some of the attributes/indicators adopted were not adequate or somehow redundant. The applications described in this paper involved a broader number of archetypes with a broader spectrum of situations that evidenced some limits of the previous implementation. For this reason, several small adjustments were undertaken in the current version (9.1).

As already set in the original formulation, sinuosity (Brierly and Fryirs [24]) was the only attribute that conceptually deserved an iteration, as it required reaches to be specified before it was computed, and these were unknown at the beginning. As an operational solution, at the first approximation stage, such reaches were assumed to coincide (as suggested within the FCT framework) by the segments connecting the flexus point of the AC axis (once smoothed to eliminate the “noise” introduced by the irregularities of the axis polyline). An improvement was introduced with a process to eliminate those segments (output of this geometric procedure) with a result shorter than the local significant length, and then we recalculated the sinuosity degree over the ensemble of the adjacent joined segments (a correction procedure that may require iterations as well and that can be conducted through a new Excel tool developed ad hoc). Once reaches are identified by the Planform–Holistic couple, the sinuosity should hence be recalculated over them and then the Planform–Holistic cycle rerun (see below regarding the Holistic).

In the original version, aside from the sinuosity degree, the indicator sinuosity type was adopted with the aim to identify in particular the Constrained sinuosity reaches. The assumption was that it would be possible to determine such an indicator by comparing the position of the AC axis with respect to the valley bottom (VB; Brierly and Fryirs [24]); i.e., whether the axis occurred to be external to it, while in the Baker application it was estimated based on expert judgment. Formalizing an automatic procedure with this aim proved however to be less straightforward than expected. Hence, a new, much simpler solution was introduced: Constrained sinuosity is a typology associated only with the single-channel family, and it appears only when the entrenchment indicator (ratio between the AC width and VB width) passes a given threshold (parameter).

Another innovation was the adoption of multiplicative scalar Value Functions (VFs) as an attempt to better discern amongst typologies (e.g., where a slice shows multiple channels, it should not belong to the single-channel family). This idea proved to result in some improvements but (as shown particularly in the Biobío case) also introduced some “hysteria” of the Planform algorithm (implemented in an Excel<sup>®</sup> Tool, version 9.1).

More importantly, it implied the necessity to work in conjunction with the Holistic categorical Tool described next; this is a kind of heuristic filter that smoothed out too-frequent variations and ensured that no final reach was shorter than the local significant length, thereby fulfilling the requirement imposed to ensure a holistic view of the river. The output of the Planform was hence input into the Holistic, and its output was the final product.

### 2.3. Introduction of the Holistic Categorical Tool Paired with the Planform Tool

The Holistic categorical algorithm (implemented in another Excel<sup>®</sup> Tool) dealt with indicators that could assume values within a discrete set, where the elements had no ordinal relationships (categorical indicators). Its philosophy is very simple: *do not leave windows shorter than  $L_M$  and assign to each stretch the prevailing value in it.*

It implements the algorithm, the main traits of which are described as follows:

*Holistic I round:*

- Identify the discontinuities of Planform type (output of Planform);



- Then, proceed from the upstream toward the downstream while considering each generic slice  $i$ .

Where there is no discontinuity, it maintains the value of the preceding slice (which in the following rounds may have been modified by the Holistic itself).

Instead, where there is a discontinuity:

- It determines the “distance of constancy  $D(i)$ ”; i.e., the number of slices along which the previous type (now changed) were kept constant within half of the significant length centered in the current slice; this distance, by construction, progressively reduces while moving to slices ahead of a discontinuity.
- “prevailing type  $K$  steps forward window”: the algorithm here identifies the most frequent type occurring within the  $K$  slices ahead.
- “prevailing type in the  $D$  residual forward window “: analogous task, but in a reduced window of just  $K - D(i) - 1$  slices ahead: this is a moving window ahead within a  $K$  horizon, the start of which is anchored to the previous discontinuity (it is changed when the algorithm processes the next discontinuity) and that progressively becomes shorter. Its purpose is to consider which value is prevailing in the vicinity in front of the current slice and so avoid it while concluding that a certain type is prevailing in the  $K$  window ahead when it indeed is, but leaving “a hole” (i.e., different types are present) in the most proximal slices:
  - When the prevailing type in this window is the same than before the (last) discontinuity  $\rightarrow$  current type was a “local hole” and therefore the previous value is maintained instead;
  - When it is “not detectable”, it is maintained;
  - Otherwise, the prevailing type within the  $K$  forward window is adopted.

*Holistic II round:*

Here, the algorithm attempts to solve the cases of reaches shorter than the local significant distance. The criterion is for the moment quite brutal: the type in these too-short reaches is just uniform with the adjacent (preceding or following depending on the user choice set at the beginning amongst the algorithm characteristics) reach type. So, the algorithm proceeds as follows:

- It identifies discontinuities in the sequence of types just determined by the Holistic I round;
- Where there is no discontinuity, it maintains the already-computed value;
- Where there is a discontinuity, if the distance  $D(i)$  from the last discontinuity is  $D(i) < K$ , it adopts the value type occurring upstream of the discontinuity; otherwise, it maintains the current one.

### 3. Case Study

#### 3.1. Study Area

The study area is located within the Biobío River basin (Figure 2). The Biobío River basin, located in the Biobío region (VIII Region) of Chile, is the second largest in the country with a surface area of 24,273 km<sup>2</sup>. It is located between parallels 36°45′–38°49′ S and meridians 71°–73°20′ W. This basin has a mixed regime and originates in the majestic Andes Mountains. As it passes through the central plain, it meanders through diverse landscapes until it finally merges with the Pacific Ocean south of Hualpén. Composed of 15 distinct sub-basins, this river system is characterized by a series of geographic and environmental conditions that contribute to its remarkable variability along its extensive course [25]. The rivers considered in this study were: part of the Biobío River itself; the Laja River, which is its main tributary; and the Duqueco river.

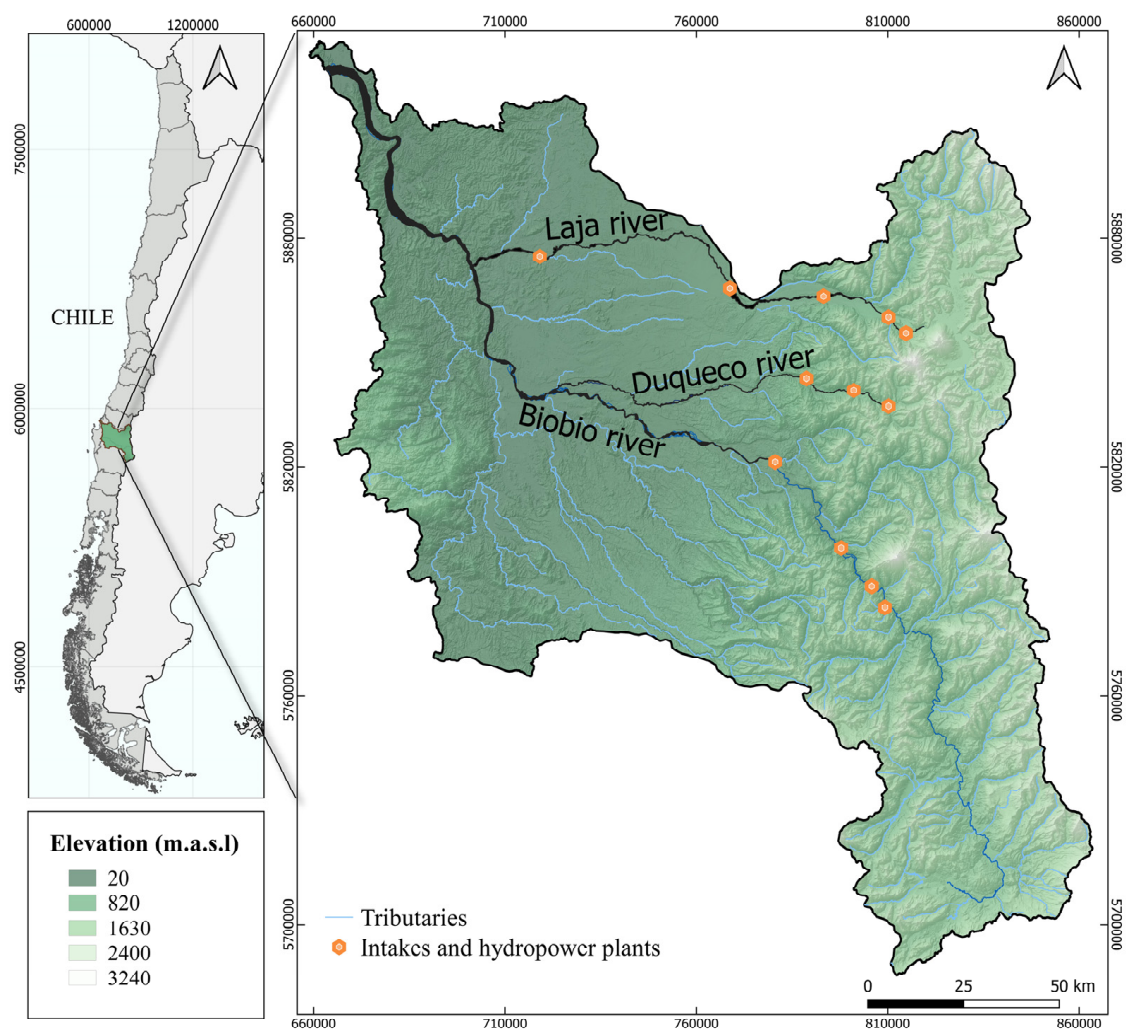


**Figure 2.** Study Area in Biobío Basin.

Originating on the eastern shore of the Gualletué Lagoon in the Andes Mountains, the Biobío River extends for approximately 380 km until it reaches its mouth [26]. For the purposes of this study, owing to the information availability, a specific long stretch of the river was selected starting from the Angostura dam, Quillaco, and running approximately 198 km to the mouth.

The Laja River, the main tributary of the Biobío River, has an area of 4667 km<sup>2</sup>. Its headwaters are in the Andes Mountains east of the Antuco Volcano and south of the “Nevados de Chillán”. This river system not only drains the Laja Lagoon but also crosses the Central Depression. Lastly, the Laja river joins with the Biobío River, marking an important confluence point [27]. Finally, the Duqueco River, which also originates in the Andes Mountains (specifically, to the southwest of the Sierra Velluda), flows toward the Biobío River, eventually converging near the town of Negrete. With a hydrographic basin of 1550.8 km<sup>2</sup> and an approximate length of 102 km (evaluated in this study), the Duqueco River has a remarkable size. Its tributaries are the Canicura, Quillaco, and Llerquenco streams, with the Coreo River as its main tributary [28]. Table 1 reports additional data on the morphometric characteristics of these rivers.

**Table 1.** Main characteristics of the rivers studied.

N	River	Year	L (km)	w <sub>max</sub> (m)	w <sub>min</sub> (m)	A. Basin (km <sup>2</sup> )	Q <sub>av</sub> (m <sup>3</sup> /s)	N. Macrosegments
1	Duqueco	2009	102	634	11	1551	55	4
2	Laja	2019	140	44	5	4667	151	5
3	Biobío	2020	198 (*)	2649	15	24,273	984	5

Notes: (\*) The length “L” of the Biobío River was analyzed from the mouth to the first dam called “Angostura” (see Figure 2). The symbol w denotes the width of the active channel envelope, “A. Basin” is the area of the basin, and “Q<sub>av</sub>” is the average flowrate.

### 3.2. Data and Methods

In this study, we utilized a high-resolution 10 m TanDEM-X radar interferometric digital elevation model sourced from the DRL (Deutsches Zentrum für Luft- und Raumfahrt—German Aerospace Center) in Germany. Complementing this dataset, satellite images from the RapidEYE and Planet Scope nanosatellite constellations were employed, offering pixel resolutions of 5 m and 3 m, respectively.

The processing of satellite images allowed the generation of Unitary Geographic Objects (UGOs) relevant to the analysis with greater efficiency than that of a manual exercise; these UGOs (or geomorphic elements) were: the active channels in high waters (i.e., including bars), the bars themselves, islands, and geomorphic units within the floodplain. To this aim, in the ENVI-IDL 5.x software, a multispectral mosaic was created using RapidEYE and Planet Scope images (for the years 2009 (Duqueco), 2019 (Laja), and 2020 (Biobío)) representing both high-water and low-water conditions within the basin. The Normalized Difference Water Index (NDWI) [29] was then computed, enabling the identification of areas with water; this distinction was achieved through spectral separation techniques specific to these materials. The geographic difference (Difference tool in QGIS) allowed us to identify those areas comprising dry soil and vegetation contained within the former; i.e., islands or bars. Subsequently, images captured on different dates reflecting varying water conditions were processed and merged to enhance the identification of islands and bars within the active channel. It must be noted, however, that this method is reliable for large rivers where hydrological changes are quite slow and hold for significant periods; for rivers like those considered here (either relatively small and/or affected by reservoir management), this method may lead to imperfect results because it is not ensured that the images—and the recorder of hydrological daily data—captured very high and low flows.

To generate the floodplain or valley bottom, we used the TanDEM-X DEM at a resolution of 10 m through the Valley Bottom Extraction Tool (V-BET) program as described in the workflow presented by Gilbert et al. [30]. V-BET is a tool that allows for the extraction and mapping of the valley bottom from a digital elevation model (DEM). Its driving idea is to identify depressed areas in a landscape by examining changes in slope within sections of the DEM transverse to the main flow direction.

Additionally, we utilized the South Rivers Toolbox tool within the QGIS 3.x interface [28] to enhance our analysis. We employed the segmentation tool offered by the “River Skeleton” module to segment the active channel and its envelope. This process involved utilizing the centerline of each UGO. It is crucial to also note that the sequencing of the centerline was essential to maintain a consistent order in the coding of the segments (Disaggregated Geographic Objects (DGOs) from upstream to downstream or vice versa.

In summary, we finally obtained through a manual exercise (conducted by students) the geomorphic elements: valley bottom (VB), active channels (ACs), and the AC envelope; and the geomorphic units (GUs): bars (bank attached left/right or point bar; mid-channel) and islands.

For planform analysis, the algorithm developed by Nardini and Brierley [11] was employed; this offered an automated approach to identify the planform characteristics. The adopted archetypes were a variant of those originally proposed by Kleinhans and Van den Berg [31]. The data eventually input into the Planform Tool were (for each slice i):

- ID of the slice or DGO (i);
- Length of discretization slice (all slices equal; 50 m was adopted for the three rivers);
- Length  $L_H(j)$  of the Hubert segment  $j(i)$  corresponding to slice  $i$  (several slices were associated with the same segment  $j$ ); reference moving window length  $L(i) = f * L_H(j(i))$ , over which the reference width  $w(j(i))$  was calculated, with  $f$  inflation factor ( $f \geq 1$ ) → corresponding significant length (smoothed)  $L_S(i) = K * w(j(i))$  with  $K$  characteristic parameter. Notice hence that  $w(j(i))$  in general did not coincide with the local slice width  $w(i)$ , which could be much more variable along the river:  $w(j(i))$  is a filtered out relative of  $w(i)$ ;
- AC envelope area (or width);
- VB area (or width);
- Area of left, right, and point bank attached bars; area of mid-channel bars;
- Number of active channels;
- Max, min, average width of low-flow water channel;
- Max and average distance between two low-flow channels (when multi-channel);
- Max whole length of water channel crossing slice  $i$  (from its departure from main channel until its joining downstream);
- Area of wetlands within the VB (for slice  $i$ );
- Sinuosity of reach in which slice  $i$  falls (see discussion above on sinuosity iteration).

Figure 3 visually presents in a comprehensive fashion the exercise conducted and the essential steps required to automatically identify the dominant archetypes governing the planform of the river within the GIS and Excel environments.

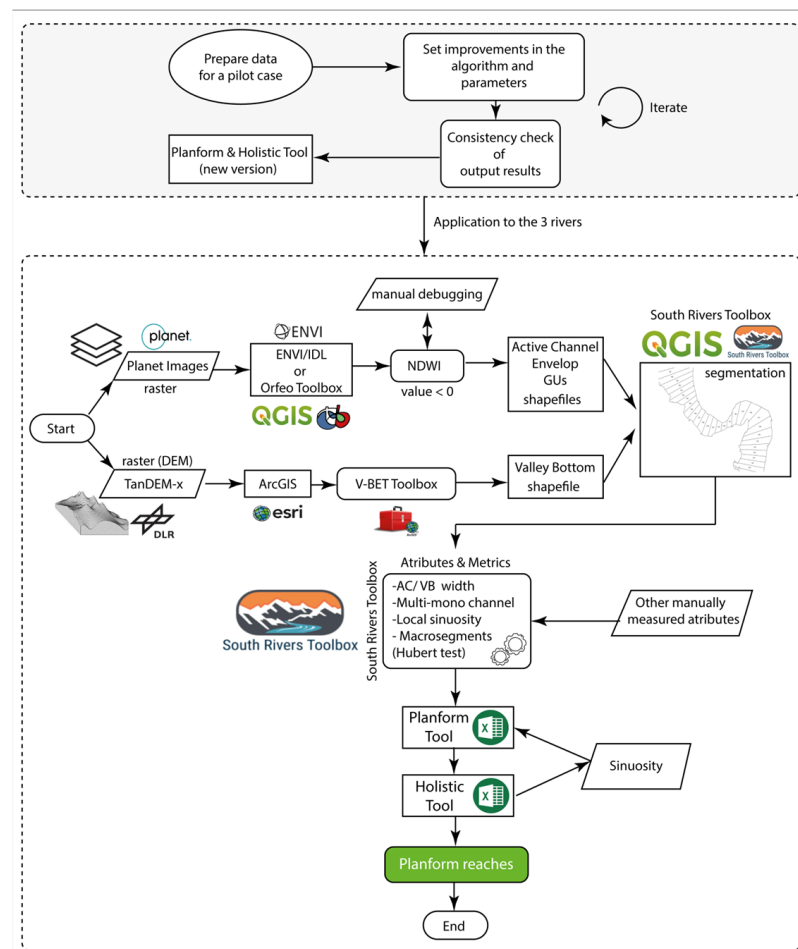


Figure 3. Workflow for calculating planform.

### 4. Results and Discussion

We do not present an expert judgment identification of Planform typology to be compared with the Tool output because the former should be the fruit of a wide exercise involving several independent experts, which has not been conducted yet. Rather, for each river we present the original geomorphic elements and units (those adopted as basic information to input into the Planform Tool), the corresponding Planform output and the final output of the Holistic. Based on such elements, the reader can verify and judge the performance of the algorithm. However, comments are provided to ease the analysis.

The important point is that all of them were obtained by using the same parametrization of the Planform; the only difference lay in the key parameter K defining the significant length, which was set to the default value of 1 for the Duqueco and Laja cases, while it was 1.5 for the Biobio case (and the T1 parameter of Holistic was consistently set to 50): this was the fruit of a couple of attempts.

The spatial discretization (segmentation) step was fixed at 50 m, which approximated the average AC envelope width of Duqueco with the idea to achieve a finer description of the units. Of course, this was an arbitrary choice that could be varied; it will be discussed later on.

#### 4.1. Duqueco River

In the stretch shown in Figure 4, the Planform and Holistic provided the same answer, which was very well suited according to the geomorphic units identified. It can be noted that some quite short reaches appeared; however, they still respected the condition of being no shorter than the local (slice i) significant length  $L_S(i)$ , as can be appreciated in Figure 5.

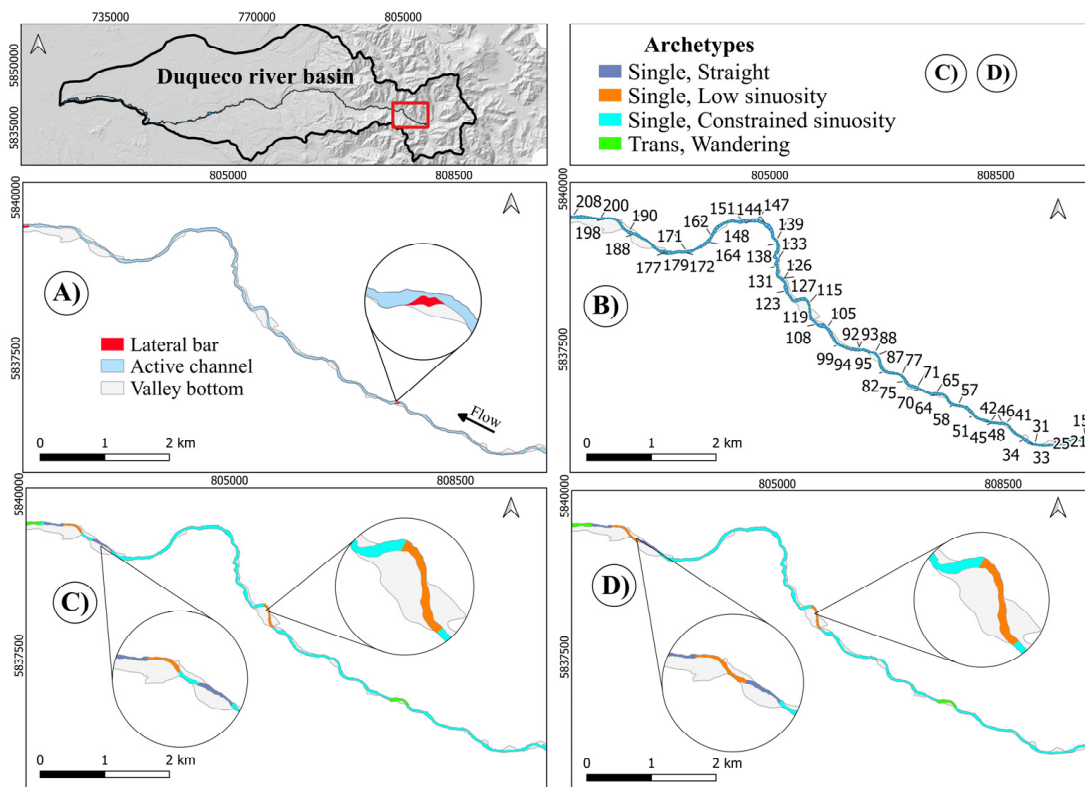


**Figure 4.** Upstream segment of the Duqueco River (slices: 15–205; slices 1–14 belong to a reservoir). Letters (A, B, ... ) identify emblematic situations along this stretch where some problems occur and/or the effect of the Holistic Tool is more evident.



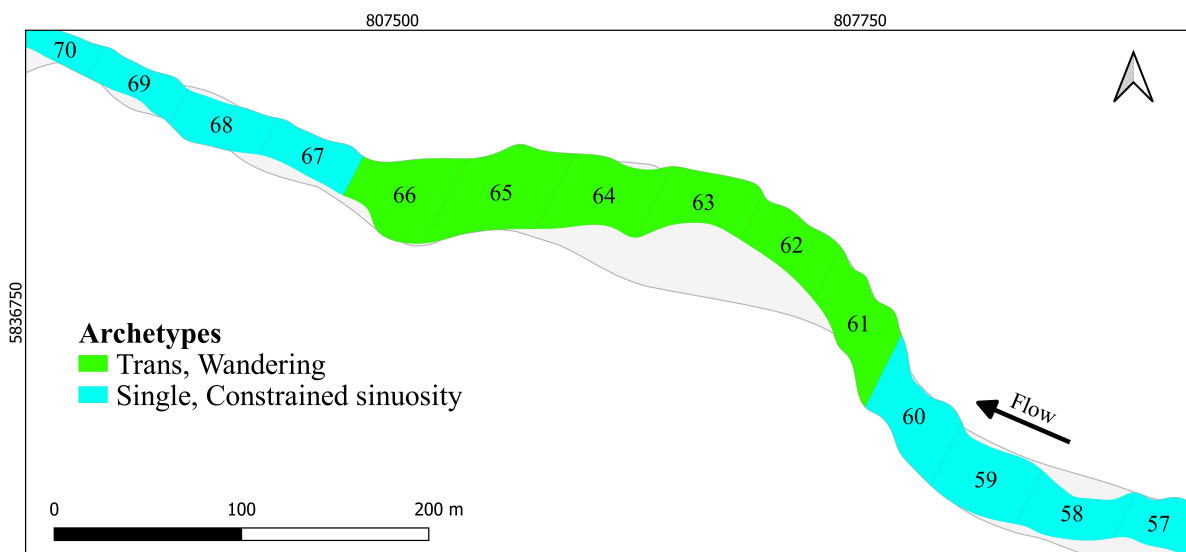


**Figure 5.** A zoom into the short reach of 61–66: it was still longer than the local significant length  $Ls(i)$  (about 300 m); the average width was around 30 m and the K factor adopted was 10. Notice that, by definition, only the archetypes from the single family could be classified as Constrained sinuosity.

As shown in Figure 6, the Planform correctly recognized a number of archetypes, including the Swallowing and the Alternate bars types, both of which belong to the Transitional family; the Swallowing had a significant enlargement with a large fluvial island inside within a prevailing single-channel reach and with no significant width difference between the two channels aside the island and no bars present. Meanwhile, the Alternate bar type required the display of a lateral bar on one side and then the opposite in an alternate fashion moving along the river without an excessive distance between any two of them (i.e., less than the significant length) and with no other bars or islands present (and hence with just a single channel) nor evident enlargement.

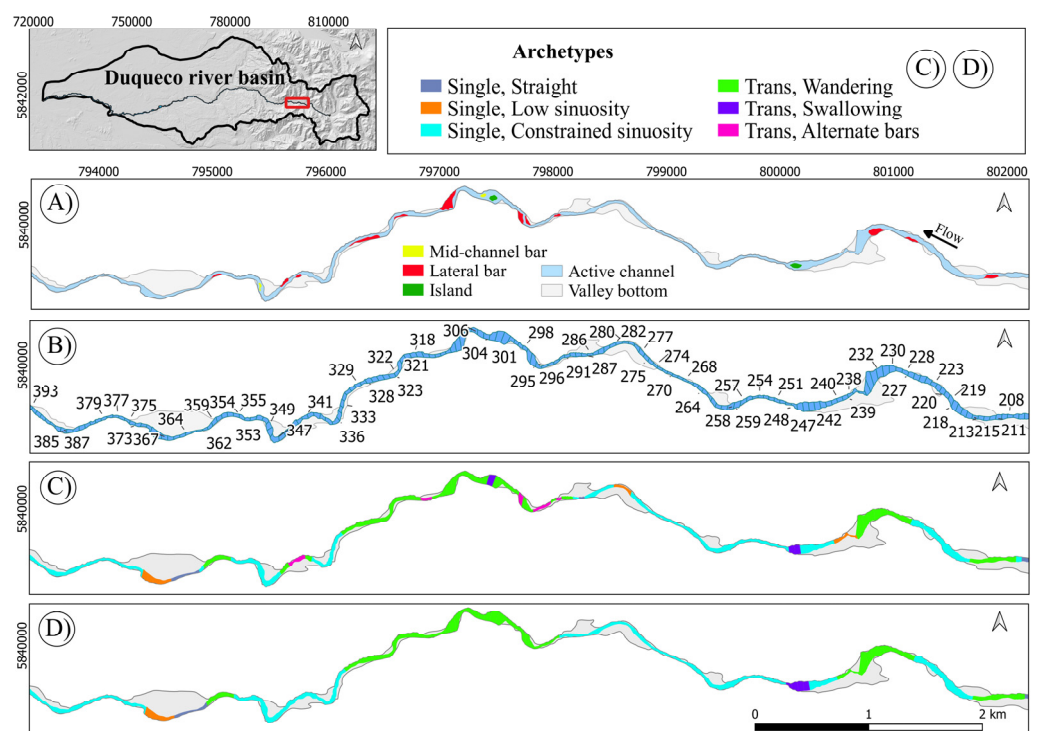


**Figure 6.** A stretch of the Duqueco River (slices: 205–370).

The Holistic, however, only maintained the first of the two Swallowing reaches (Figure 6): this was the effect of a special functionality introduced to avoid to skip such reaches because Swallowing reaches are typically shorter than the significant length and are a kind of anomaly, but they nevertheless deserve to be identified. Therefore, as soon as at least two consecutive Swallowing slices were found, it added a short queue before and after such a nucleus to ensure it acquired a sufficient consistency. In this case, this occurred only in the upstream Swallowing reach because it was born sufficiently long (more than just one slice), while this was not the case for the other reach, which hence disappeared.

The Alternate bar reaches were correctly identified, but they proved to be too short according to the local significant length criterion, and hence they were overcome by the prevailing local type. An analogous destiny was given to other too-short reaches identified by the Planform but was correctly merged with “the mainstream” by the Holistic.

In the stretch shown in Figure 7, again the Planform correctly recognized several archetypes, including the Swallowing and the Alternate bar types. The Holistic respected them except for the too-short reaches that included in particular the ALT bars (ones that hence disappeared), but the Swallowing one was correctly maintained (according to the criteria illustrated above), although an excessive queue was added. It can also be noticed that two single-channel reaches in the middle (between slices 461 and 481) were differentiated because the downstream one of the two was a Constrained sinuosity according to the criteria adopted.

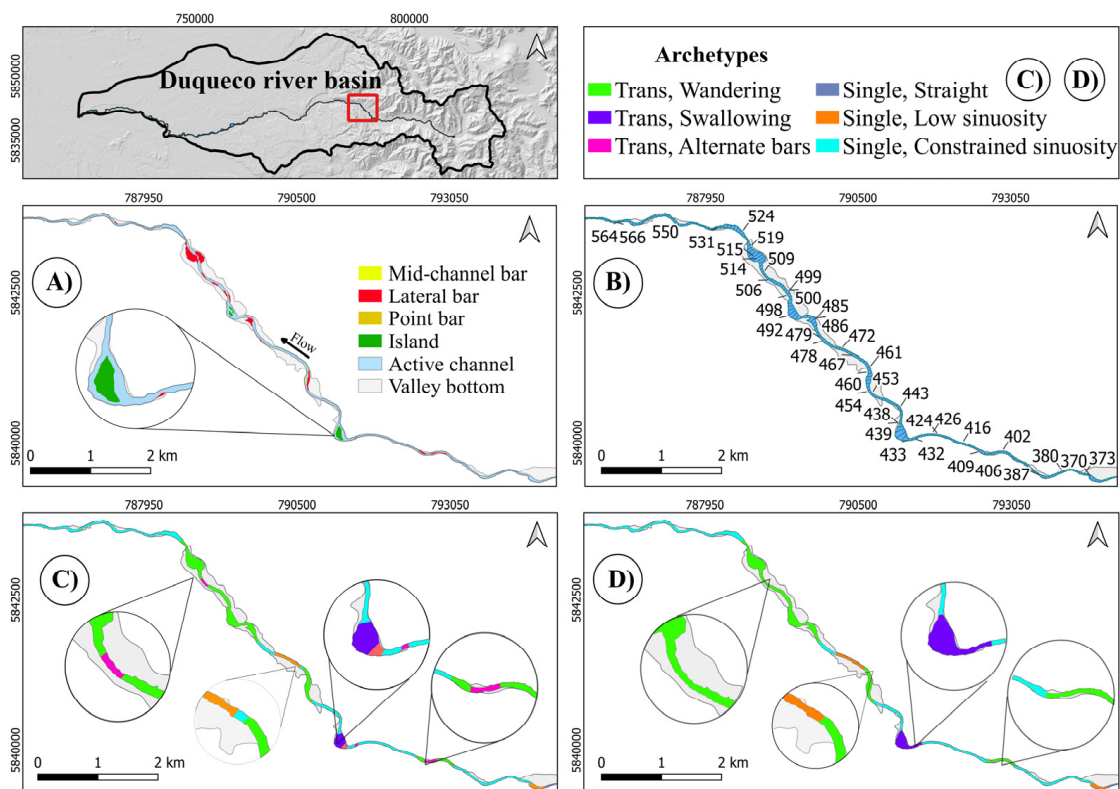
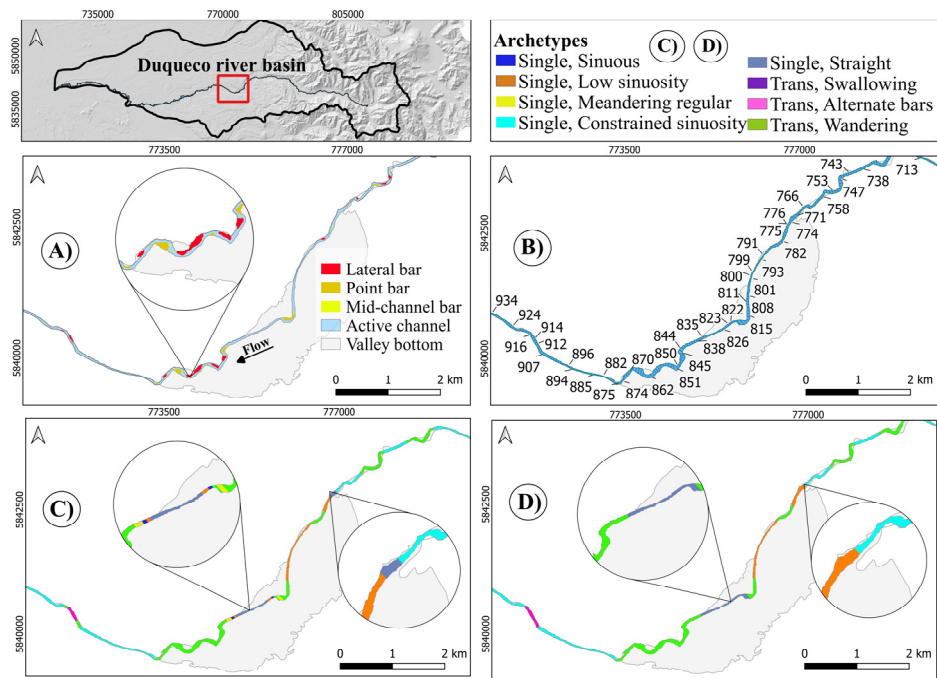


Figure 7. A stretch of the Duqueco River (slices: 370–562).

As shown in Figure 8, again the Holistic showed its utility by eliminating a few too-short reaches. It conserved on the other side the ALT bar reach, although it arbitrarily extended it a bit outside of the actual reach delimited by the alternating bars (notice that the downstream bar is small and not very visible in this image but is well presented).



**Figure 8.** A stretch of the Duqueco River (slices: 725–926); notice that an upstream stretch was omitted because it was banal (fully Constrained sinuosity).

As shown in Figure 9, the behavior was very similar to the previous case with some imperfections in the position of the start and end of the ALT bar reaches that nevertheless were correctly identified.

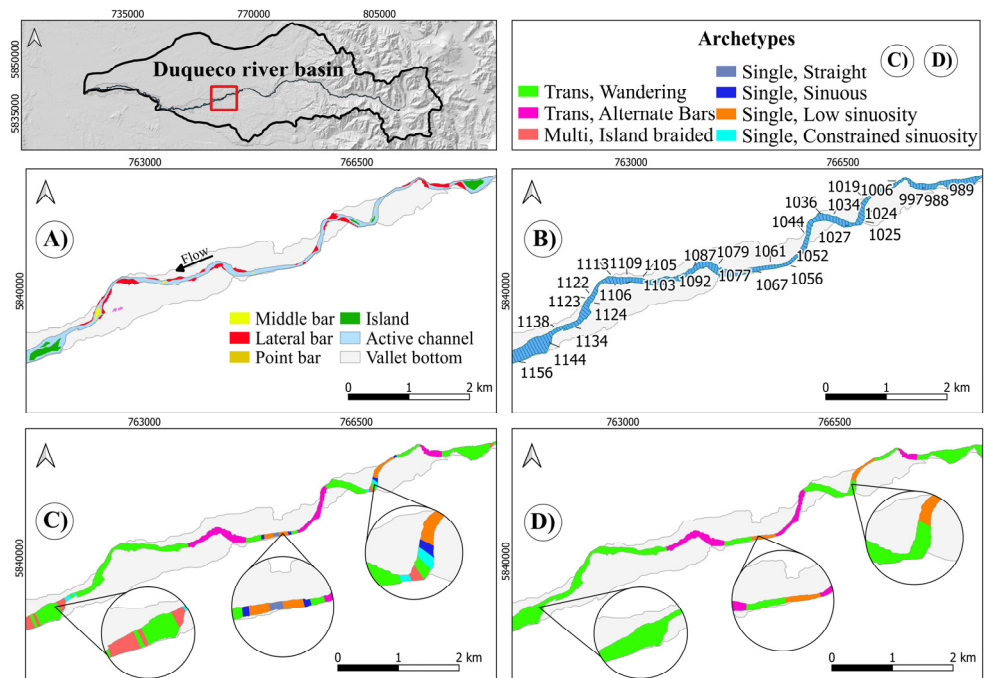


**Figure 9.** A stretch of the Duqueco River (slices: 982–1151).

As shown in Figure 10, the function of the Holistic was more evident, and the results were very acceptable. A new type correctly appeared, although just for two reaches (1532–1536 and 1567–1587): the Single Meandering archetype. Also, the stretch 1455–1474 might seem to be meandering, but the widespread presence of bars and islands correctly

placed it in the Trans Wandering category; additionally, the sinuosity did not achieve the 1.5 threshold.

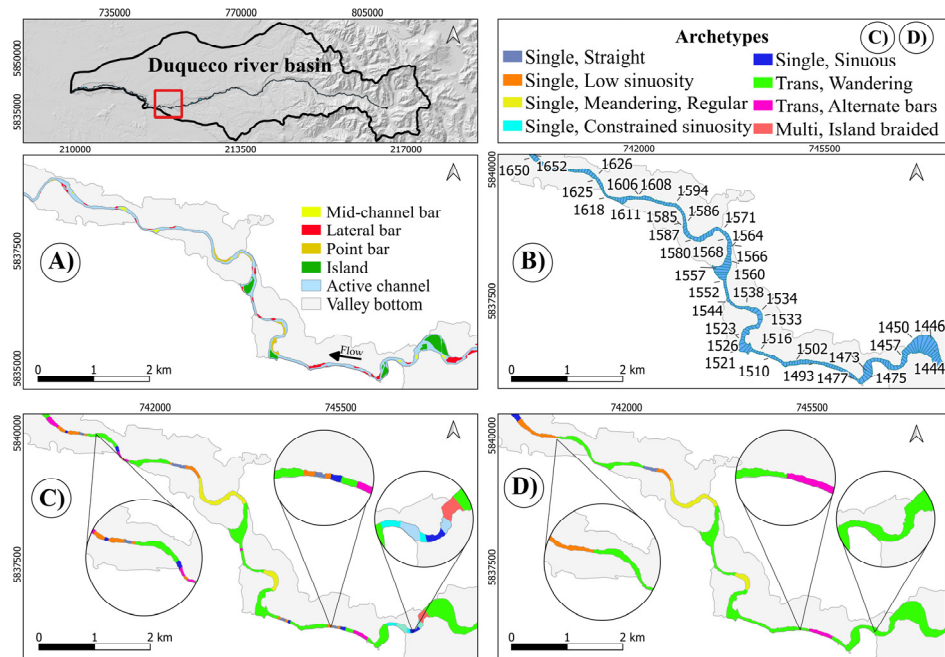


**Figure 10.** A stretch of the Duqueco River (slices: 1440–1657) after a long Trans Wandering reach was correctly identified.

As shown in Figure 11, the Planform correctly identified several archetypes, including a Swallowing reach, although there was some imprecision in the ALT bar ones. The Holistic fulfilled its duty by eliminating too-short reaches and added some further correction, although it added an excessive queue to the Swallowing.

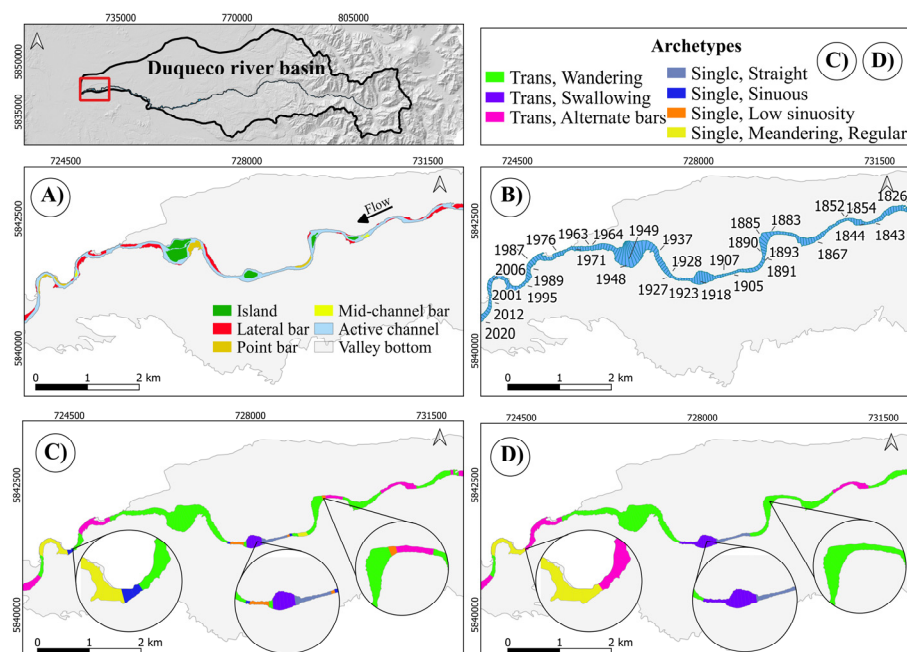


**Figure 11.** The final stretch of the Duqueco River (slices: 1834–2016).



### 4.2. Laja River

In the stretch shown in Figure 12, the Planform correctly distinguished the Single, Low sinuosity; the Constrained sinuosity; and the Single, Straight reaches, while the Holistic correctly eliminated some very short reaches.

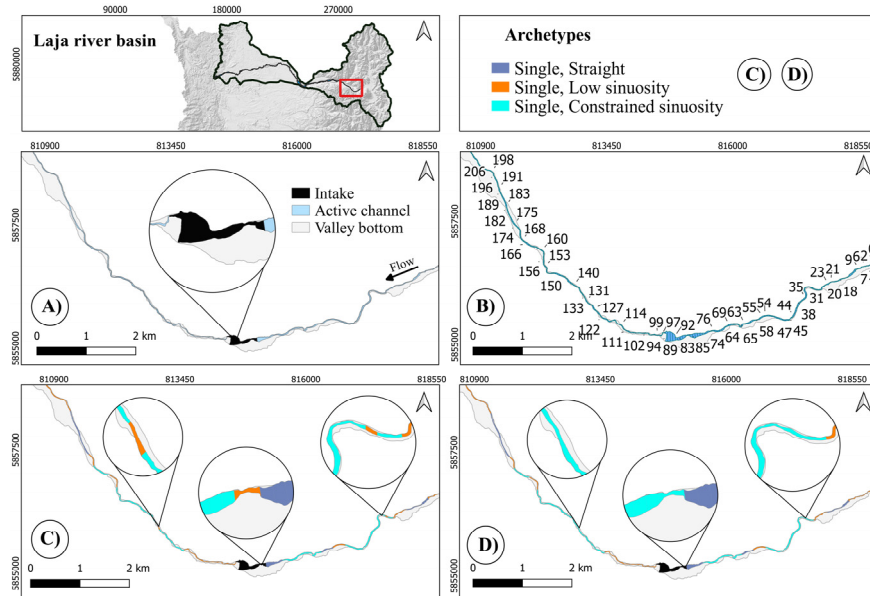


Figure 12. The first upstream stretch of the Laja River (slices: 10–194).

Figure 13 shows a quite varied stretch where the Planform identified several types, alternating where probably several choices might appear somehow questionable; in particular, the Swallowing one (because there was not a very marked enlargement while there was a rather significant difference in the width of the two channels). The Holistic correctly eliminated some very short reaches (all those kept indeed were longer than their local significant length) and, consistent with its criteria, maintained the Swallowing reach, with this probably being the only questionable final choice. In other words, it greatly improved the Planform response.

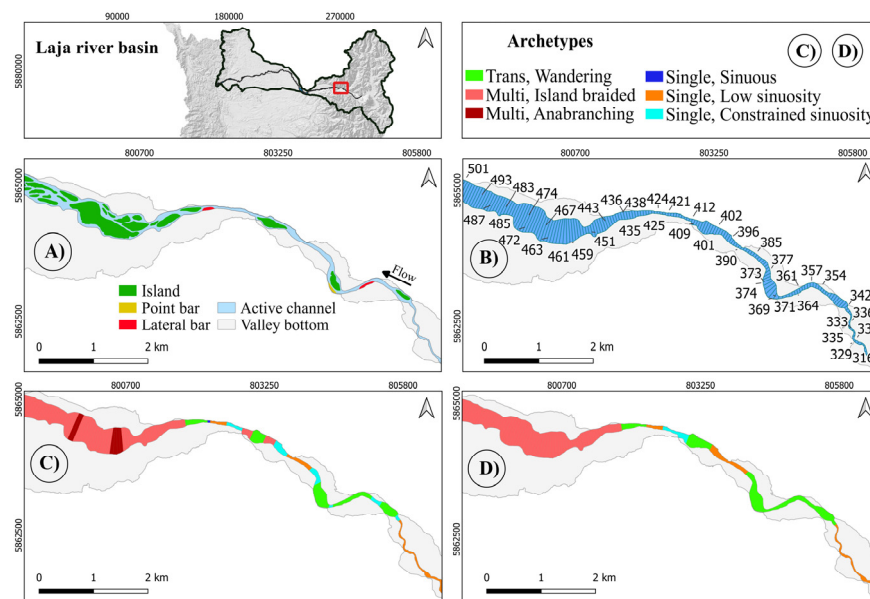
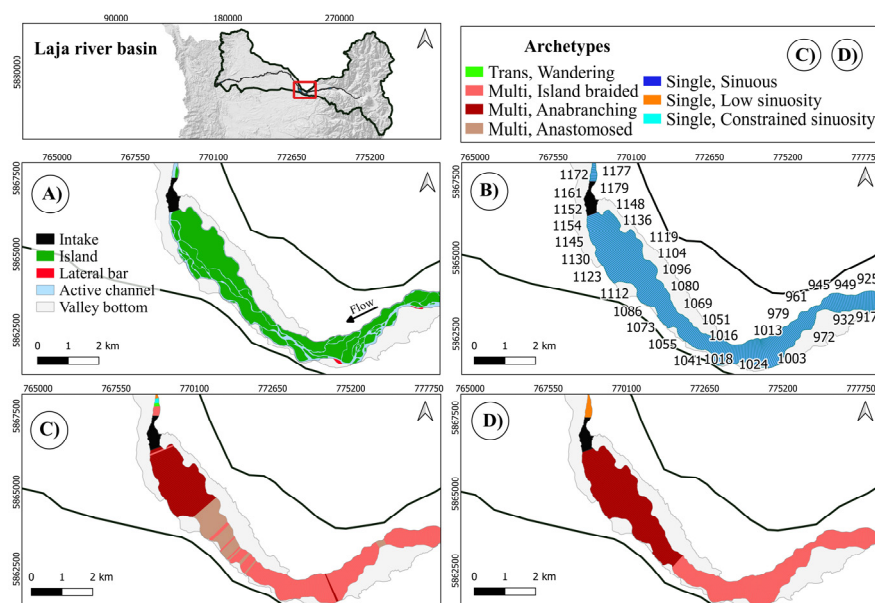


Figure 13. Another stretch of the Laja River (slices: 318–499) skipping an intermediate stretch very similar to the previous one.



This stretch (Figure 14) also included very different situations because of the presence of a reservoir (grey zone), which in large part was responsible for the dramatic widening occurring upstream of it. Of the many reaches identified by the Planform, the Holistic maintained a reasonable selection, including the Trans, Swallowing one. The latter might seem unjustified at first sight, but at a closer view indeed it is justified by the significant enlargement, although mainly with respect to the downstream reach (the algorithm currently does not check, as it should, that the enlargement does occur in both sides) and the presence of a two almost equally wide branches. Both Tools split the stretch upstream of the reservoir in the first (downstream) part into Multi, Anabranching according to the presence of very large lateral branches and a significant enlargement; while more upstream, a second part was classified as Multi, Island braided because the characteristics just mentioned were smoothed there. The ALT bars' reach was canceled, while the Swallowing one was (consistently) maintained, although an excessive queue was attached.



**Figure 14.** Another stretch of the Laja River (slices: 947–1263) skipping an intermediate stretch that was quite uniform (mainly Multi, Island braided).

It is worth noting that here the algorithm was applied without splitting the river (although the presence of the reservoir would suggest doing so), so it certainly was bit confused by the grey area that input misleading information.

According to the Planform, the stretch in Figure 15 included several different types, including Multi, Island braided; Single, Low sinuosity, Straight, Meandering Regular, and Constrained sinuosity; and Trans, Wandering and ALT bars (two reaches). The presence of a quite rare Meandering reach was justified—according to the criteria specified in the algorithm—by the presence of a point bar (which, rigorously speaking, could be highly questionable, but is what was given in input to the algorithm, so it is left out of the discussion here) and a sufficient value of the sinuosity itself (higher than 1.5).

The Holistic significantly reduced this geomorphic diversity, and probably most of the readers will be in favor of its choices. Indeed, several were too short and as such were eliminated, like the first (upstream) ALT, while the second was kept and enlarged a bit (possibly unduly).

In Figure 16, the river presents a significant enlargement just upstream of a bottleneck (naturally imposed here). A significant Single, Constrained sinuosity reach was correctly identified by both the Planform and Holistic, while upstream and downstream of it, multichannel reaches were present. The reach upstream of the bottleneck was identified as Anabranching according to the criteria specified; i.e., a significant enlargement (particularly

with respect to the following reach), very large side channels, a significant difference in width amongst the multiple channels, and the absence (or negligible presence) of bars.

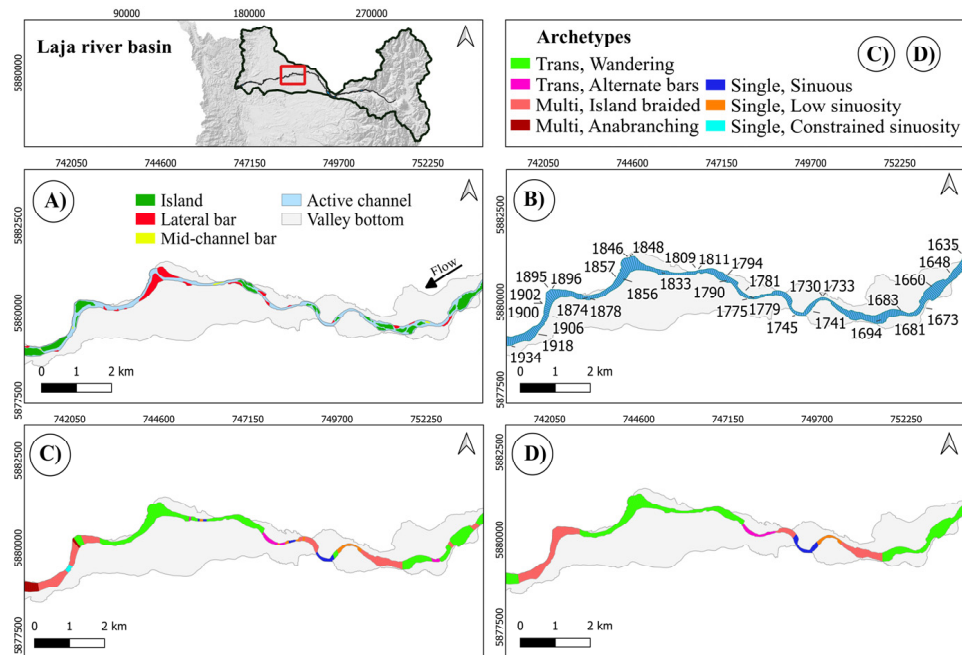


**Figure 15.** A quite varied stretch of the Laja River (slices: 1634–2121) skipping an intermediate stretch that was much more regular and well represented.

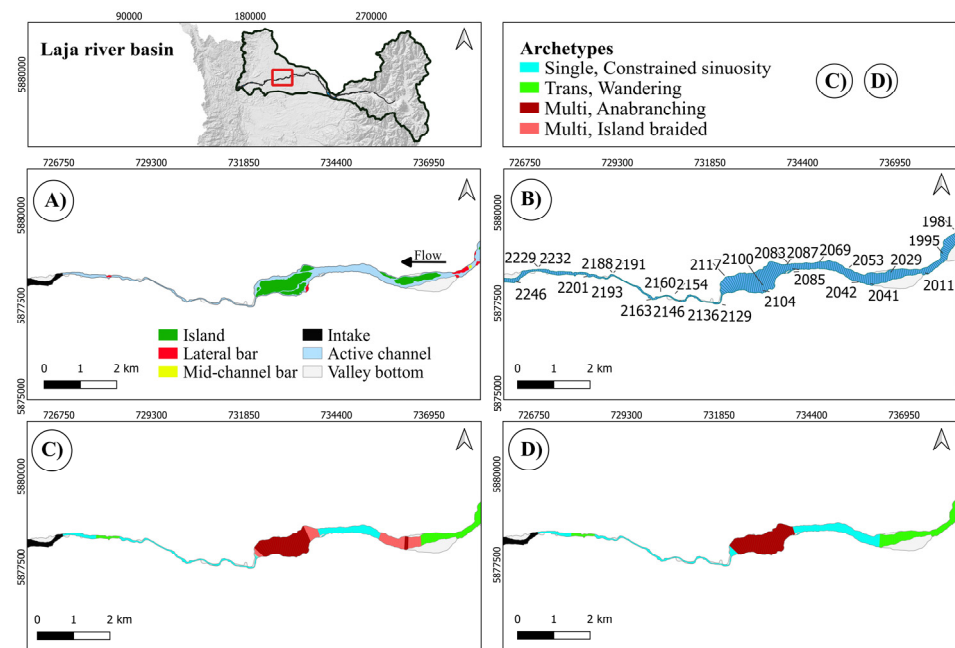


**Figure 16.** The last interesting stretch of the Laja River (slices: 1982–2225).

### 4.3. Biobío River

Notice that in this case, the numbering of slices began from the most downstream slice, contrary to the other cases.

Figure 17 shows that the sporadic presence of relatively small islands did not suffice to switch to the multichannel family. The reach on the right was correctly identified as Constrained sinuosity, although it improperly involved few slices on the left that were not (3876–3858). Although a Swallowing slice appeared in the Planform, because it was

isolated, it was then correctly ignored by the Holistic. The differentiation between the last two reaches (both single channels) was correctly based on the value for the sinuosity.

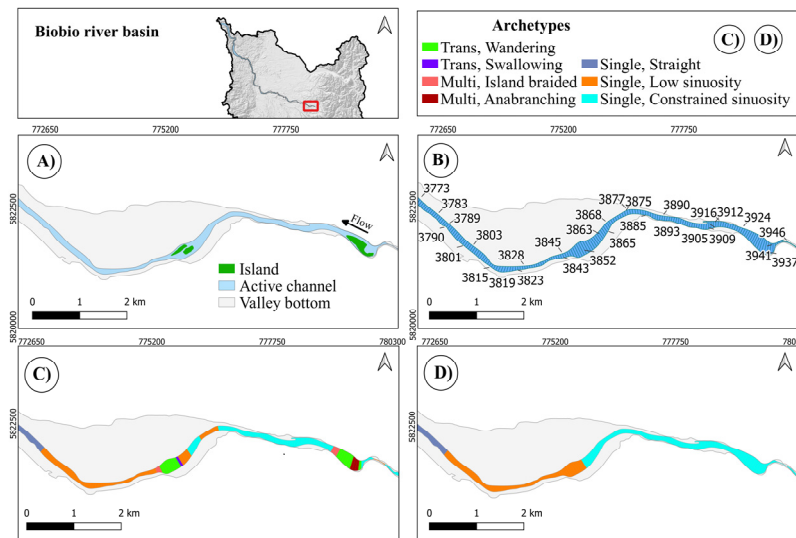


**Figure 17.** Upstream segment of the Biobío River (slices: 3950–3779; notice that in this case the numbering of slices began from the most downstream slice, contrary to the other cases).

As shown in Figure 18, the algorithm demonstrated moderate performance by accurately identifying the primary typologies but imprecisely defined the position of the reaches: in particular, the Single, Low sinuosity reach (of about 3.2 km length) should have started earlier (at slice 3506, but it started at 3485, which is about a kilometer after) and ended earlier (at slice 3448 rather than slice 3426; i.e., 1.1 km earlier). This was evidently a mistake by the Holistic and was associated with a non-optimal choice of the significant length factor *K*. The key factor distinguishing the Anabranching from the Island braided archetype was the presence in the former of a channel of significant length, the marked presence of a main channel, as well as the presence of an enlargement of the active channel envelope.

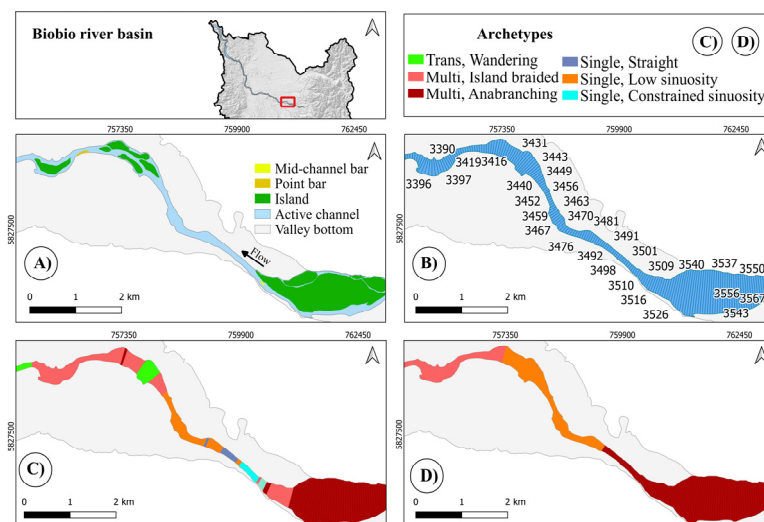


**Figure 18.** Biobío River (slices: 3554–3373).

In Figure 19, it is evident that the algorithm performed well because it correctly captured the main typologies and sufficiently correctly defined the position of the reaches. It was apparent that the Planform’s key role of filtering out the uncertainties (or hysteresis) was definitely exaggerated, at least with respect to previous versions of the Tool we

experienced. This suggested that the use of multiplicative VF should be rethought and at least moderated.

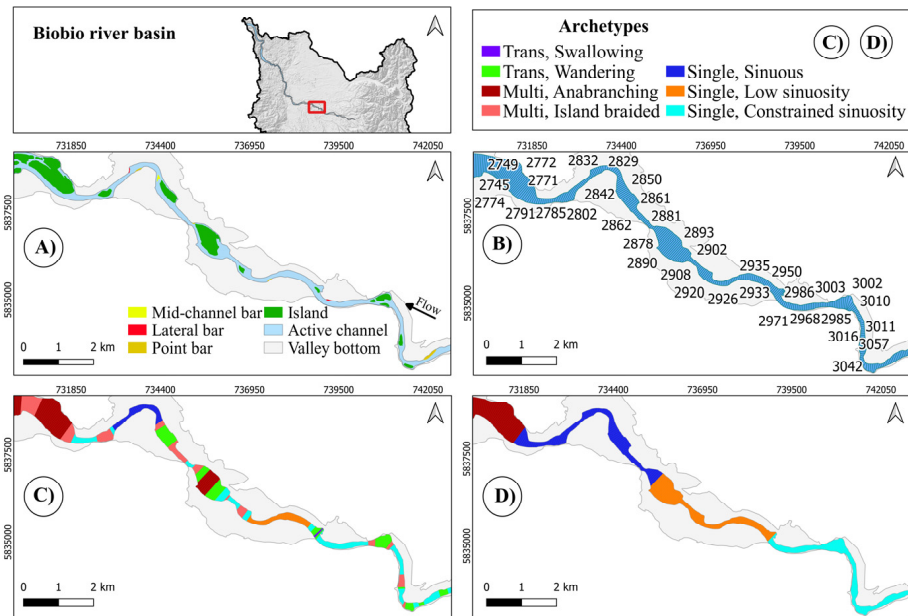


Figure 19. Biobío River (slices: 3056–2756).

Figure 20 shows again that the algorithm performed quite well despite the hysteria of the Planform. The only mistake was the identification of a Swallowing reach, but this was due to a technical detail that will be discussed later.

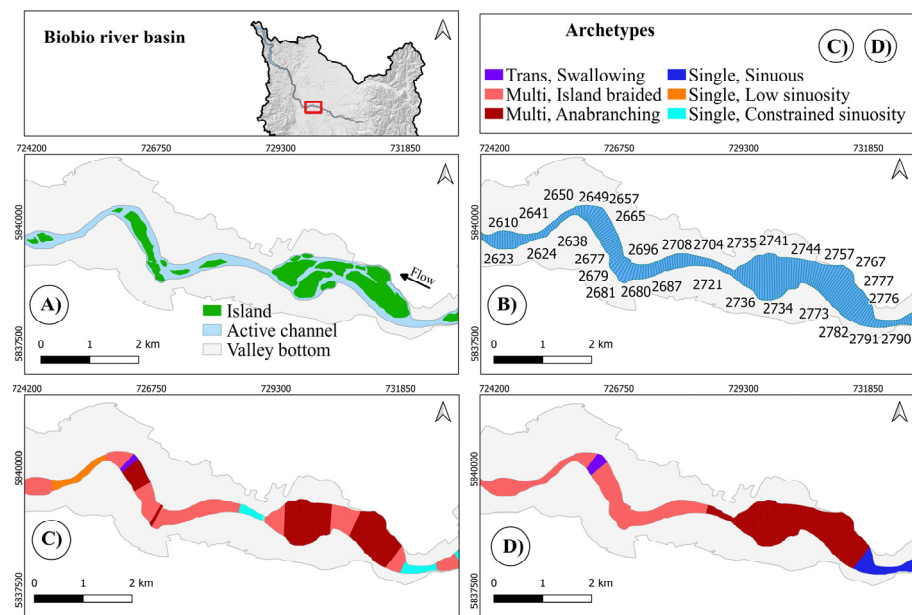
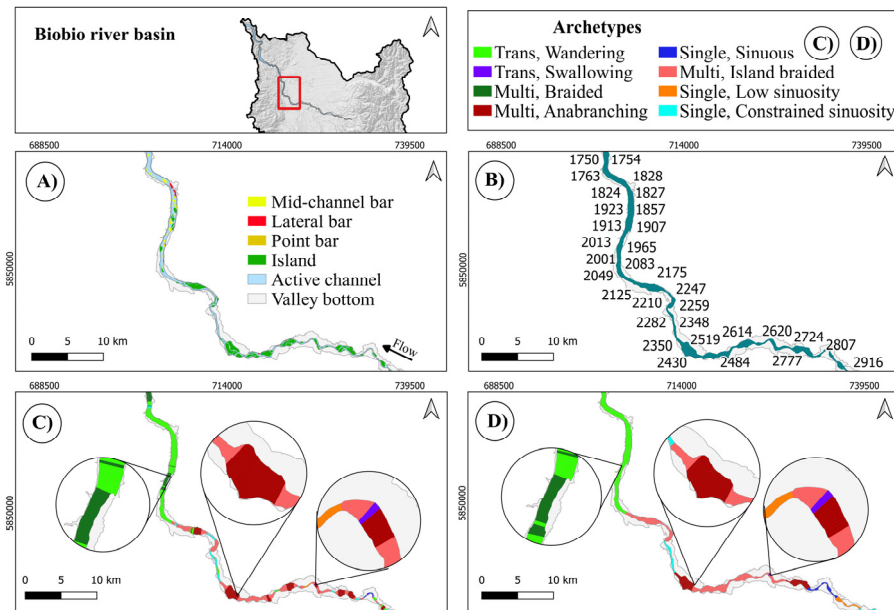


Figure 20. Biobío River (slices: 2790–2617).

The output shown in Figure 21 was consistent with the geomorphic evidence (the Swallowing reach was the same as noted above and commented upon later on), although it could be questionable where it was appropriate to identify Anabranching reaches: here, the Holistic only retained two of the multiple smaller reaches identified by the Planform because only those constituted a significant length and indeed presented all the due characteristics, as already mentioned previously. The new Wandering transitional archetype

appeared at the downstream end (top left) as several lateral bars appeared, which denied the Island braided typology.



**Figure 21.** Biobío River (slices: 2880–1751). This is a view at a smaller scale to better appreciate the response of the algorithm to a longer distance.

In the situation reported by Figure 22, the algorithm had to deal with the difficult task of interpreting the assemblages of multiple small islands and bars. The Planform, although with a significant uncertainty, correctly identified specific sub-reaches with the Braided, Wandering, Island braided (and even, very locally, Constrained sinuosity) archetypes. The Holistic, under the compelling requirement to eliminate reaches shorter than the significant length, merged two braided sub-reaches by incorporating an island zone that at first sight should not have been part of it. However, taken from another point of view, that island sub-reach was too short to deserve identification as an actual reach, and no other archetype would fit better to the unified reach. So, the choice of the Holistic was hardly improvable.

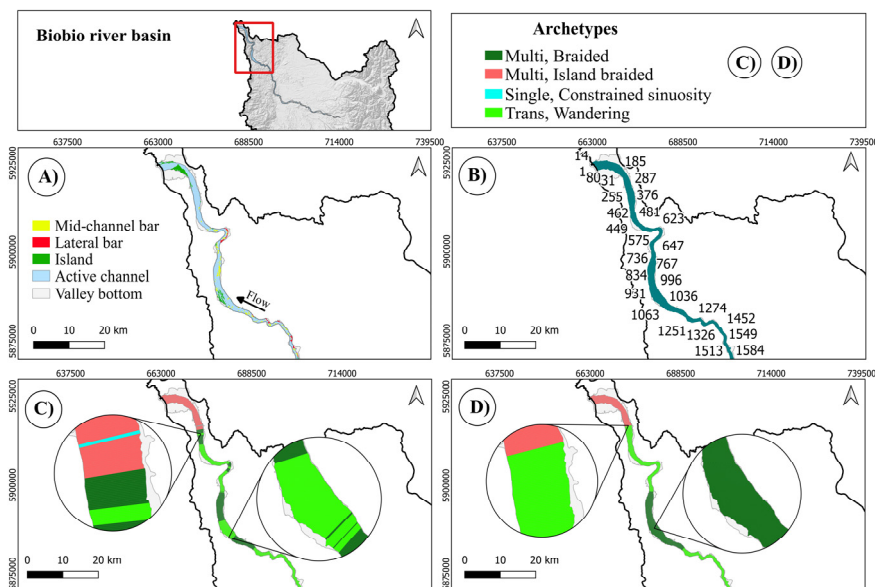


**Figure 22.** Biobío River (slices: 1542–0001): another view at a smaller scale because variations here were less frequent.



#### 4.4. General Considerations

It is worth observing that the ability of the algorithm was not only identifying the most suited archetype but also deciding the reach to be assigned to a given archetype. This was not a trivial task, and the algorithm seemed to perform well, although certainly it was not perfect. Several dams were present along the considered rivers, but this fact was ignored in this application, thereby introducing a certain bias in the results. A practical (although approximate) recipe to avoid this type of difficulty is easy, however: just break the river into (two) stretches at each dam site and proceed with each one separately.

Figure 23 shows a statistical summary of the percentage of total length of each river according to the dominant Planform archetypes for the three rivers.

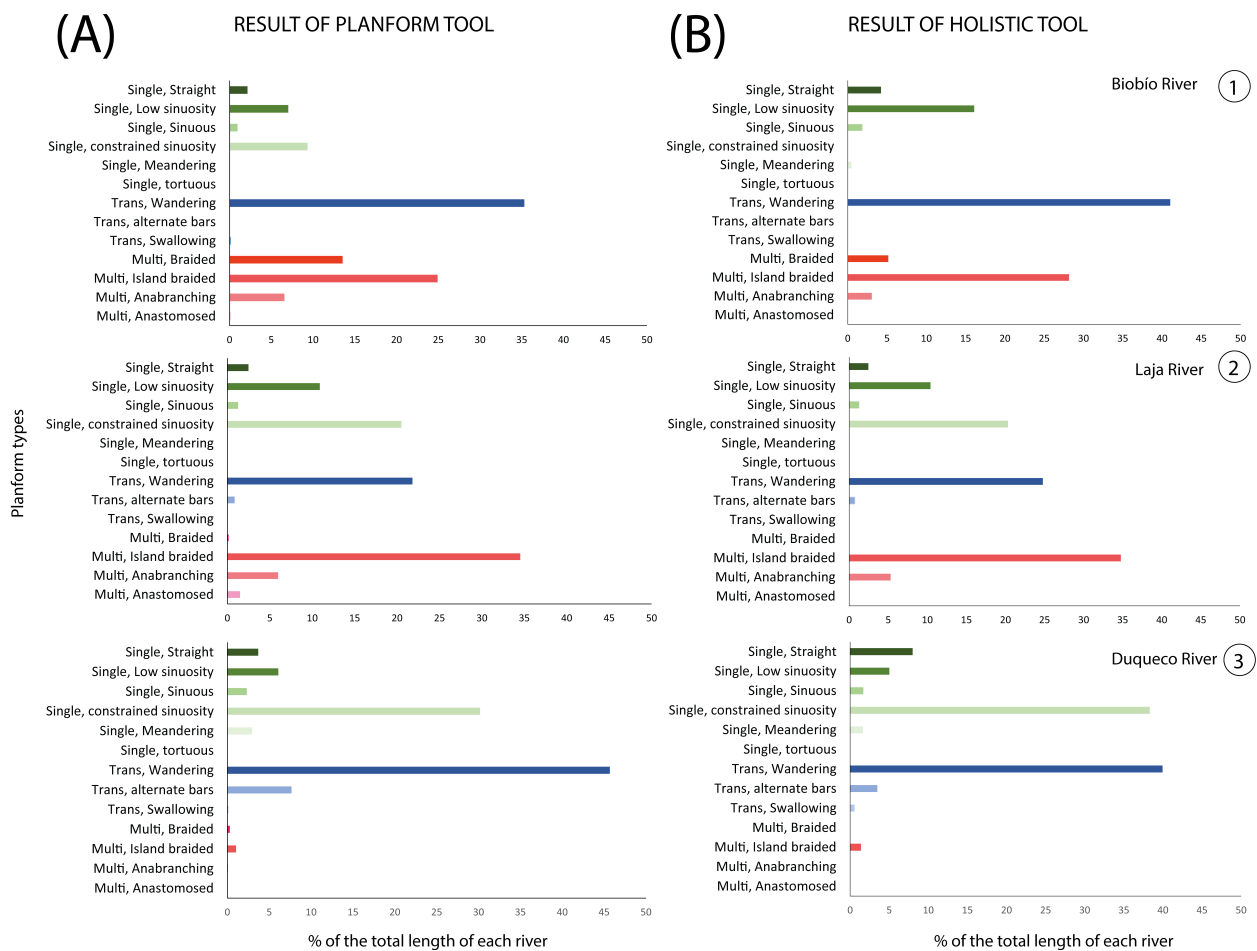


**Figure 23.** Main planform archetypes determined with the automated methodology by the Planform Tool and the Holistic Tool, respectively, for the (1) Biobío River, (2) Laja River, and (3) Duquenco River. The three main groups of archetypes (Planform types) are differentiated by colors: (a) Singles (green shades); (b) Trans (blue shades) and (c) Multi (red shades). As already discussed in the text, the output of the Planform algorithm (A) could exhibit some “hysteria” owing to frequent variations in the classified archetypes; the Holistic Tool implemented a heuristic filter able to smooth out such variations (B) while taking care that no final segment was shorter than the locally significant distance.

The Biobío case was quite challenging. It indeed presented a somewhat confused physical configuration amongst multiple small islands and bars, probably owing to anthropogenic alterations linked to deforestation in its catchment. On the other side, the width along the whole river varied greatly (compare, for instance, slices 3810 in Figure 17 and 2767 in Figure 19), and this indeed presented a quite difficult challenge for the algorithm: in order to discretize with a sufficient resolution the narrowest segments, a slice length of

50 m was suitably adopted, but this proved to be very tiny when moving downstream. In fact, the too-thin character of the slices together with the multiplicative Value Functions adopted introduced a marked hysteresis of the algorithm as consecutive slices apparently contained very different situations. In addition, a problem arose with the Swallowing archetype: as already explained, the algorithm hence had a special functionality to preserve such reaches (which were not very long by definition): it added a short queue before and after the nucleus found; in the Biobío case (Figure 24), a couple of such adjacent slices were indeed found just because the slices were very thin, and otherwise just one would show up. This fact resulted in a Swallowing reach being identified where it should not have been.

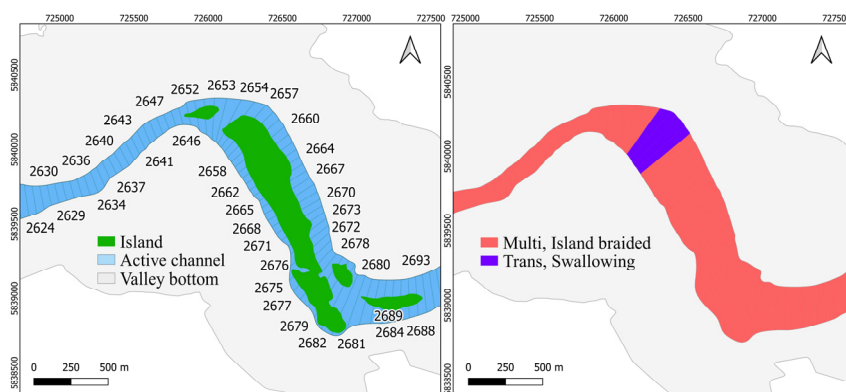


**Figure 24.** False identification of a Swallowing reach in the Biobío River (slices: 2656–2659).

Also, the Duqueco case also was quite challenging because it presented sudden, significant enlargements and quite a large number of archetypes; nevertheless, the algorithm basically captured them all. In that case, however, a weakness of the Holistic appeared: as at the end of Round I, still few reaches were present that were shorter than the significant length; it then proceeded through Round II and applied a last-option rule with which it assigned to the too-short reach the same typology of the following one: this produced the undue preceding queue that was classified as Swallowing, which it should not have been (this can be corrected in future versions).

The Meandering type appeared very rarely; while visually we would like perhaps to have seen it more often; but this was consistent with the criterion that a Meandering required a sinuosity not less than 1.5.

## 5. Conclusions

The proposed Tool (indeed, the Planform–Holistic couple) performed quite satisfactorily, and the exercise proved what had been theorized in the Discussion section by Nardini and Brierley [11]; i.e., that a given parametrization would hold for different rivers because all the differences were captured explicitly by the attributes considered. Only the key parameter  $K$  determining the significant length (and its associated minimum length parameter  $T1$  of the Holistic) possibly deserved an adaptation given a specific case study, but a couple of attempts could be sufficient.

However, the algorithm can still be improved: better sets of attributes and corresponding indicators can be adopted; more precise identifications of the start and end for the ALT bar type can be set; improved Value Functions can be introduced; and particularly, the role of the multiplicative ones rediscussed and marginalized to avoid the unpleasant hysteresis they introduce. In the Holistic, the manner in which the special case of Swallowing type was dealt with can be improved to avoid excessively long queues appearing, and the appearance—although quite unusual—of reaches not fulfilling the significant length constraint should be avoided, perhaps by iterating the same algorithm once more. It must be considered, however, that the imprecisions or mistakes related to the whole river length were quite minor indeed.

Another line of improvement refers to the introduction of new archetypes. This is certainly possible; however, addressing very large rivers (e.g., the Amazon, Magdalena, Ob, Mackenzie, Congo, and Orinoco rivers described in Ashworth and Lewin [32]) would raise new demanding challenges because each one of the multiple channels may require a specific identification with specific geomorphic units.

An interesting experiment would be to receive several different expert identifications of planform reaches/types and compare their consistency with the algorithm answer.

Another experiment would be the use of an ML algorithm fed on the same information basis (the indicators values associated with the spatial discretization) to ascertain what the answer would be in the unsupervised mode (analogous to the one adopted here) and then in the supervised mode once expert judgments were available.

Although the Planform and Holistic Tools were developed on an Excel® platform, the whole package was conceived to be potentially fully automatized once the basic geomorphic elements and units are provided (a task that itself can potentially be conducted in an automatized way similar to, for instance, that used in [8,19,28]). However, difficulties are present, like the ability to determine for each discretization slice the length of the water channels intercepted or the initial estimation of the sinuosity (which itself requires an iterative procedure).

From an operational point of view, it is recommended to split the cases with excessively marked width differences along the river into two (or more) long stretches and adopt a proportional discretization length; i.e., in particular for the Biobío River, a length greater than the 50 m now adopted; the same recommendation holds when an artificial structure like a dam is present.

The exercise has an intrinsic value in making explicit the criteria to classify reaches amongst the available archetypes. It ensures a consistent application of such criteria, a property (consistency) that can hardly be ensured by expert judgment. However, its direct usefulness lies in:

- The ability to characterize large river networks;
- The possibility of carrying out a regular, systematic monitoring of a river network to detect possible typological changes as clear indicators of (natural or anthropogenic) alterations that have occurred.

**Author Contributions:** Conceptualization, A.G.C.N. and S.Y.; methodology, A.G.C.N. and S.Y.; software, F.S., N.V., Z.C. and R.R.; validation, A.G.C.N. and S.Y.; formal analysis, F.S., N.V., Z.C. and R.R.; investigation, A.G.C.N. and F.S.; resources, S.Y.; data curation, A.G.C.N. and S.Y.; writing—original draft preparation, A.G.C.N. and F.S.; writing—review and editing, S.Y., F.S. and A.G.C.N.; visualization, Z.C.; supervision, S.Y., A.G.C.N. and J.V.-B.; project administration, S.Y.; funding acquisition, S.Y. and J.V.-B. All authors have read and agreed to the published version of the manuscript.

**Funding:** This study was funded by the South Rivers Toolbox project (19BP-117424) funded by CORFO.

**Data Availability Statement:** All raw data can be provided by the corresponding authors upon request.

**Acknowledgments:** We would like to thank Planet for providing the RapidEYE and Planet Scope (nanosatellite) images used in this study free of charge as well as the TanDEM-X DEM GEOL08450 project for providing the high-spatial-resolution terrain elevation model.

**Conflicts of Interest:** The authors declare no conflict of interest.

## References

1. Kondolf, G.M.; Piégay, H.; Schmitt, L.; Montgomery, D.R. Geomorphic classification of rivers and streams. In *Tools in Fluvial Geomorphology*; Wiley: Hoboken, NJ, USA, 2016; pp. 133–158. [[CrossRef](#)]
2. Buffington, J.; Montgomery, D. Geomorphic classification of rivers. In *Treatise on Geomorphology*; Shroder, J., Wohl, E., Eds.; Elsevier: San Diego, CA, USA, 2013; Volume 9, pp. 730–767.
3. Fryirs, K.; Brierley, G. *Practical Applications of River Styles Framework as a Tool for Catchment-Wide River Management: A Case Study from Bega Catchment New South Wales*; MacQuirie University: Auckland, New Zealand, 2005.
4. Nardini, A.; Yépez, S.; Mazzorana, B.; Ulloa, H.; Bejarano, M.D.; Laraque, A. A systematic, automated approach for river segmentation tested on the Magdalena River (Colombia) and the Baker River (Chile). *Water* **2020**, *12*, 2827. [[CrossRef](#)]

5. Parker, C.; Clifford, N.J.; Thorne, C.R. Automatic delineation of functional river reach boundaries for river research and applications. *River Res. Appl.* **2012**, *28*, 1708–1725. [[CrossRef](#)]
6. Piégay, H.; Arnaud, F.; Belletti, B.; Bertrand, M.; Bizzi, S.; Carbonneau, P.; Dufour, S.; Liébault, F.; Ruiz-Villanueva, V.; Slater, L. Remotely sensed rivers in the Anthropocene: State of the art and prospects. *Earth Surf. Process. Landf.* **2020**, *45*, 157–188. [[CrossRef](#)]
7. Dallaire, O.C.; Ouellet Dallaire, B.; Lehner, R.; Sayre, M. Thieme A multidisciplinary framework to derive global river reach classifications at high spatial resolution. *Environ. Res. Lett.* **2018**, *14*, 024003. [[CrossRef](#)]
8. Demarchi, L.; Bizzi, S.; Piégay, H. Hierarchical object-based mapping of riverscape units and in-stream mesohabitats using LiDAR and VHR imagery. *Remote Sens.* **2016**, *8*, 97. [[CrossRef](#)]
9. Bernard, T.G.; Davy, P.; Lague, D. Hydro-geomorphic metrics for high resolution fluvial landscape analysis. *J. Geophys. Res. Earth Surf.* **2022**, *127*, e2021JF006535. [[CrossRef](#)]
10. Jézéquel, C.; Oberdorff, T.; Tedesco, P.A.; Schmitt, L. Geomorphological diversity of rivers in the Amazon Basin. *Geomorphology* **2022**, *400*, 108078. [[CrossRef](#)]
11. Nardini, A.; Brierley, G. Automatic River Planform identification by a logical-heuristic algorithm. *Geomorphology* **2021**, *375*, 107558. [[CrossRef](#)]
12. Frasson, R.P.d.M.; Pavelsky, T.M.; Fonstad, M.A.; Durand, M.T.; Allen, G.H.; Schumann, G.; Lion, C.; Beighley, R.E.; Yang, X. Global relationships between river width, slope, catchment area, meander wavelength, sinuosity, and discharge. *Geophys. Res. Lett.* **2019**, *46*, 3252–3262. [[CrossRef](#)]
13. Beechie, T.; Imaki, H. Predicting natural channel patterns based on landscape and geomorphic controls in the Columbia River basin, USA. *Water Resour. Res.* **2014**, *50*, 39–57. [[CrossRef](#)]
14. Beechie, T.J.; Liermann, M.; Pollock, M.M.; Baker, S.; Davies, J. Channel pattern and river-floodplain dynamics in forested mountain river systems. *Geomorphology* **2006**, *78*, 124–141. [[CrossRef](#)]
15. Rabanaque, M.P.; Martínez-Fernández, V.; Calle, M.; Benito, G. Basin-wide hydromorphological analysis of ephemeral streams using machine learning algorithms. *Earth Surf. Process. Landf.* **2022**, *47*, 328–344. [[CrossRef](#)]
16. Bertrand, M.; Piégay, H.; Pont, D.; Liébault, F.; Sauquet, E. Sensitivity analysis of environmental changes associated with riverscape evolutions following sediment reintroduction: Geomatic approach on the Drôme River network, France. *Int. J. River Basin Manag.* **2013**, *11*, 19–32. [[CrossRef](#)]
17. Guillon, H.; Byrne, C.F.; Lane, B.A.; Sandoval Solis, S.; Pasternack, G.B. Machine learning predicts reach-scale channel types from coarse-scale geospatial data in a large river basin. *Water Resour. Res.* **2020**, *56*, e2019WR026691. [[CrossRef](#)]
18. Horacio, J.; Ollero, A.; Pérez-Alberti, A. Geomorphic classification of rivers: A new methodology applied in an Atlantic Region (Galicia, NW Iberian Peninsula). *Environ. Earth Sci.* **2017**, *76*, 746. [[CrossRef](#)]
19. Bizzi, S.; Lerner, D.N. Characterizing physical habitats in rivers using map-derived drivers of fluvial geomorphic processes. *Geomorphology* **2012**, *169*, 64–73. [[CrossRef](#)]
20. Donadio, C.; Brescia, M.; Riccardo, A.; Angora, G.; Veneri, M.D.; Riccio, G. A novel approach to the classification of terrestrial drainage networks based on deep learning and preliminary results on solar system bodies. *Sci. Rep.* **2021**, *11*, 5875. [[CrossRef](#)]
21. Alber, A.; Piégay, H. Spatial disaggregation and aggregation procedures for characterizing fluvial features at the network-scale: Application to the Rhône basin (France). *Geomorphology* **2011**, *125*, 343–360. [[CrossRef](#)]
22. Nardini, A.; Yépez, S.; Bejarano, M.D. A Computer Aided Approach for River Styles—Inspired Characterization of Large Basins: A Structured Procedure and Support Tools. *Geosciences* **2020**, *10*, 231. [[CrossRef](#)]
23. Hubert, P. The segmentation procedure as a tool for discrete modeling of hydrometeorological regimes. *Stoch. Environ. Res. Risk Assess.* **2000**, *14*, 297–304. [[CrossRef](#)]
24. Brierley, G.; Fryirs, K. *Geomorphology and River Management: Applications of the River Styles Framework*; Blackwell Publishing: Malden, MA, USA, 2005. [[CrossRef](#)]
25. Caamaño, D. Caracterización de cambios morfológicos en la parte media del río Biobío. Master's Thesis, Universidad Católica de la Santísima Concepción, Concepción, Chile, 2019.
26. Niemeyer, H. Hoyas hidrográficas de Chile: 8a. Región del Bío-Bío, 9a. Región de la Araucanía, 10a. Región de Los Lagos. 1980. Available online: <https://bibliotecadigital.ciren.cl/handle/20.500.13082/2348> (accessed on 1 February 2023).
27. Mardones, M.; Vargas, J. Efectos hidrológicos de los usos eléctrico y agrícola en la cuenca del río Laja (Chile centro-sur). *Rev. Geogr. Norte Gd.* **2005**, *33*, 89–102.
28. Yépez, S.; Salas, F.; Nardini, A.; Valenzuela, N.; Osoreo, V.; Vargas, J.; Rodríguez, R.; Piégay, H. Semi-automated morphological characterization using South Rivers Toolbox. *Proc. IAHS* **2023**, *100*, 1–8.
29. McFeeters, S.K. The use of the Normalized Difference Water Index (NDWI) in the delineation of open water features. *Int. J. Remote Sens.* **1996**, *17*, 1425–1432. [[CrossRef](#)]
30. Gilbert, J.T.; Macfarlane, W.W.; Wheaton, J.M. The Valley Bottom Extraction Tool (V-BET): A GIS tool for delineating valley bottoms across entire drainage networks. *Comput. Geosci.* **2016**, *97*, 1–14. [[CrossRef](#)]

31. Kleinhans, M.G.; van den Berg, J.H. River channel and bar patterns explained and predicted by an empirical and a physics-based method. *Earth Surf. Process. Landf.* **2011**, *36*, 721–738. [[CrossRef](#)]
32. Ashworth, P.J.; Lewin, J. How do big rivers come to be different? *Earth-Sci. Rev.* **2012**, *114*, 84–107. [[CrossRef](#)]

**Disclaimer/Publisher's Note:** The statements, opinions and data contained in all publications are solely those of the individual author(s) and contributor(s) and not of MDPI and/or the editor(s). MDPI and/or the editor(s) disclaim responsibility for any injury to people or property resulting from any ideas, methods, instructions or products referred to in the content.